# Acoustic Emission based Crack Tracking for Concrete Structures

Zhang, F.; Yang, Y.

**Publication date**
2019

**Document Version**
Accepted author manuscript

**Published in**
Journal of Acoustic Emission

**Citation (APA)**
Zhang, F., & Yang, Y. (2019). Acoustic Emission based Crack Tracking for Concrete Structures. In M. A. Hamstad, & G. Manthei (Eds.), *Journal of Acoustic Emission: Proceedings of International Conference on Acoustic Emission - 9* (Vol. 36, pp. S159-S164). Article 36-S159 Acoustic Emission Group. http://www.aewg.org/jae/JAE-Vol_36-2019-4C.pdf

# Acoustic Emission based Crack Tracking for Concrete Structures

Fengqiao Zhang*[a],.Yuguang Yang[a]
[a] Delft University of Technology, the Netherlands

## ABSTRACT

Acoustic Emission (AE) monitoring is one of the possibilities to detect the crack distribution in existing concrete structures. However, the conventional method requires further destruction like opening of new cracks or propagation of the existing cracks. In this paper, a new strategy of using local cumulative AE activities during unloading to track the crack trajectory is proposed. With this strategy, a relatively low load level which does not cause further destruction to the structure is needed. The possibility of this strategy is experimentally examined using a real-scale beam of 10-ton damaged under cyclic loading. For calibration, the crack opening is measured by Digital Image Correlation (DIC). The crack patterns detected by the new strategy and DIC show good agreement.

**Keywords:** concrete beam, cyclic loading, Acoustic Emission, source localization, crack tracking.

## 1. INTRODUCTION

The safety of the large stock of aging existing concrete structures is important to the society. As a key link in the maintenance of these structures, the present conditions including the crack distribution have to be evaluated accurately. At the moment, effectively evaluating the crack distribution inside the structures remains challenging. One of the available possibilities is to use Acoustic Emission (AE) technique [1,2]. In the conventional method, application of AE requires opening of new cracks or further propagation of the existing cracks, which is linked to heavier loading of the structures towards its ultimate limit state. Usually this is recognized as proof loading test of the structures [3], which requires heavy loading equipment with high cost. In this paper, a different strategy on crack tracking is proposed. In the proposed approach, a relatively low magnitude of load is applied to open the existing cracks. The AE activities during the crack closure is used to track the trajectories of the cracks.

The new strategy is validated by a large scale lab test of a 10-ton reinforced concrete beam. For calibration, the crack development is analyzed by Digital Image Correlation (DIC) measurement. The result of this paper provides the possibility of AE based crack tracking in the assessment of the present conditions of the existing concrete structures.

## 2. AE BASED CRACK TRACKING

### 2.1 AE activity during unloading

For concrete structures with cracks, it was shown that during unloading, the closure of the existing cracks or the friction between rebar and concrete, etc. may lead to the AE activities [4,5]. In order to make use of the AE activities during unloading, the expression Calm Ratio was proposed by Ohtsu et al. in [5,6], which was defined as the ratio of the cumulative AE activities during unloading to that of the whole cycle. In a later study reported by Yang et al. [4] on beams from an existing concrete bridge, it was found that the calm ratio is proportionally linked to the crack opening. The observations suggest that the AE activities during unloading can be used as an indication of the presence of existing cracks.

### 2.2 AE source localization and error estimation

As a widely applied algorithm, grid search method is employed in the study to determine the location of the AE signal source [1]. The basic principle of the algorithm is to compare the calculated arrival time difference from the estimated location and the observed arrival time difference from the measurement [7].

Factors involved in the algorithm such as the choice of arrival time picking methods and the presence of cracks influence on the travel times of the signal, thus induce an offset between the estimated source location and the real source location, which is defined as source localization error in [8]. According to Zhang, considering an arrival time picking error within 5 μs and a crack with an opening in range of [0.05 3] mm between the source and the receiver, the source localization error was around 15 cm in a target area of 1m × 1m. This amount of source localization error should be taken into account in the AE based crack tracking in concrete structures.

### 2.3 Local cumulative AE activities

In the study of Ohtsu et al. [5,6] and Yang et al. [4], the relationship between AE activities and the crack opening were studied at global level across the height of the whole specimen. Similar relationship is expected at the level of the crack trajectory locally. In this paper, a term local cumulative AE activities is proposed. The AE activities during unloading located in each cell are counted as the local cumulative AE activities during unloading. Here, cells are discretized measuring area. The size of the cell determines the accuracy of the crack tracking but is limited by the AE source localization error. This approach of using local cumulative AE activities during unloading to track the crack pattern is referred to as AE based crack tracking. It cannot only locate the existing cracks, but also indicate the local crack opening along its trajectory.

## 3. EXPERIMENT

To explore the AE source localization on real-size structural members, a test on a 10-ton reinforced concrete beam with length of 10 m, height of 1.2 m, and width of 0.3 m was conducted. The concrete had a nominal compressive strength of 65 MPa. The maximum aggregate size was 16 mm. Reinforcing bars in the beams were 6ϕ25, with concrete cover of 25 mm. The beam was simply supported with a span of 9 m and loaded by a point load at 3 m from one support (Figure 1).

The beam was loaded cyclically shown in Figure 2. The first seven load cycles are marked as L1-L7. After the beam was loaded to 250 kN in L5, two smaller magnitudes of load (L6 and L7) were applied on the beam to reproduce the practical condition that structures in service can be deteriorated due to heavier loads before the assessment.

Fourteen AE sensors of R6I-AST with a central frequency of around 60 kHz were installed on the south side of the beam to record the AE hits (Figure 1). The hits with the peak amplitude over 60 dB were selected to do the source localization. In the source localization, the arrival times were based on the threshold crossing method where the threshold was set to be 45 dB in the data acquisition system.

On the north side of the beam, a sprinkle pattern was painted to do the DIC displacement measurement. Since the boundary conditions of the beam is plain stress, the crack distribution at the two side surfaces can be assumed as constant in the width direction of the specimen. Therefore, the measured crack development from DIC can be used to calibrate the AE source localization results.

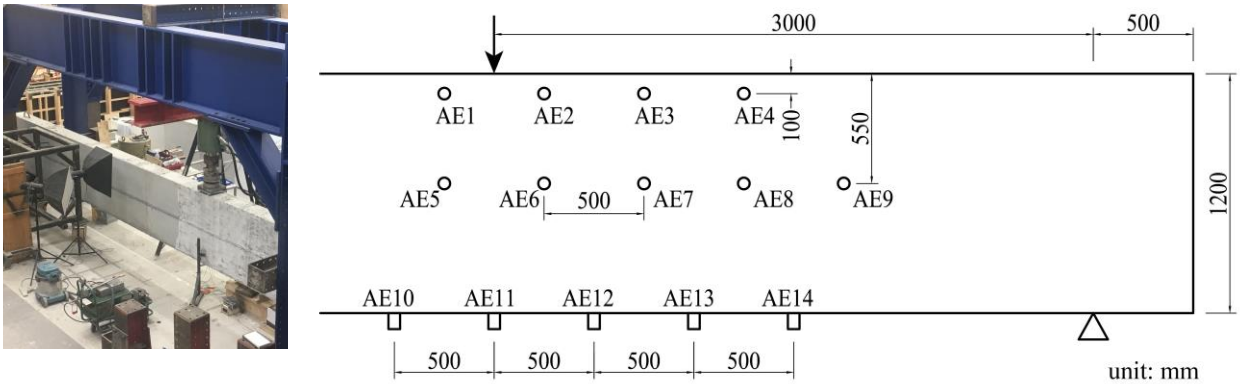


**Figure 1: (left) test setup and (right) AE sensor layout on the back side**

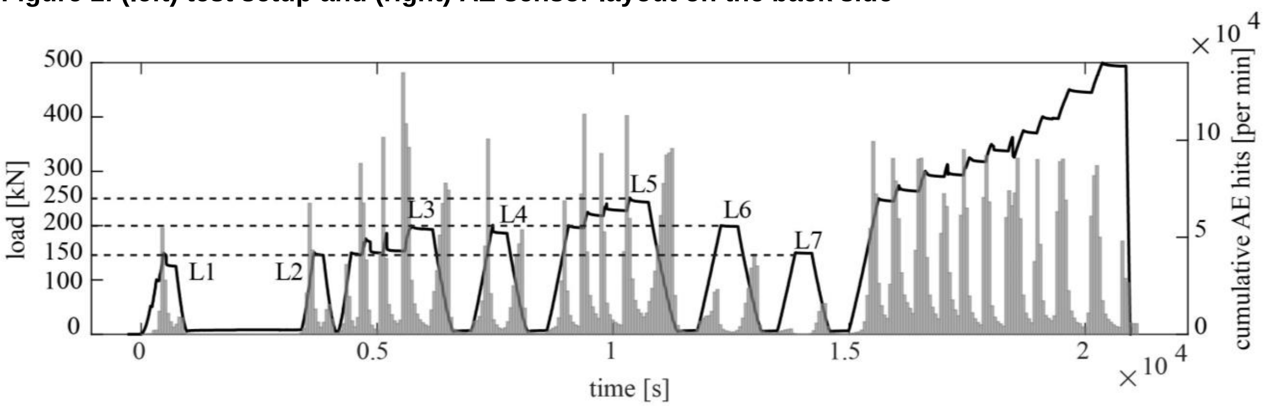


**Figure 2: loading history combined with the cumulative AE hits per minute; the load cycles of interest are marked as L1-L7**

## 4. RESULTS

### 4.1 Crack development

In the three-point bending test, the gradient of the bending moment resulted in a gradual propagation of the bending cracks with the increase of the load level. Crack patterns at different load levels have been obtained by DIC. The crack pattern at 250 kN in L5 is shown in Figure 3 (left) as an example in which the five cracks reaching the neutral axis of the specimen were studied further and marked as C2-C6. The crack C1 was marked because it was the first initiated crack (in L1). Consequently, C2, C3, C4, and C5 occurred in L3, and C6 occurred in L5. During the load cycles L6 and L7, no new cracks were observed.

The crack opening along its trajectory was determined using DIC output. Measuring points were selected on the profile of the crack (C4 shown in Figure 3, right, as an example). The short line at each point indicates the local normal direction. The crack opening was calculated by checking the displacement difference between the two points in the normal direction of the crack locally.

The opening of the cracks C3 and C4 at 200 kN (L6) and 150 kN (L7) from the previous unloaded condition is shown in Figure 4. It can be found that the re-opening of the existing crack was proportionally linked to the applied load. For the crack opening along its trajectory, in general, the crack opening was wider in the bottom part than that at the crack tip. While, due to the opening of the secondary cracks near the crack C4 in the bottom, the crack opening of C4 below 0.3 m is limited. In this study, the lower bound of the DIC measurement is assumed to be 0.05 mm due to the resolution limitation. Therefore, according to the DIC measurement, C3 hardly opened in L6 and opened towards a height of around 0.3 m in L7; C4 opened towards a height of around 1 m and 0.9 m in L6 and L7, respectively.

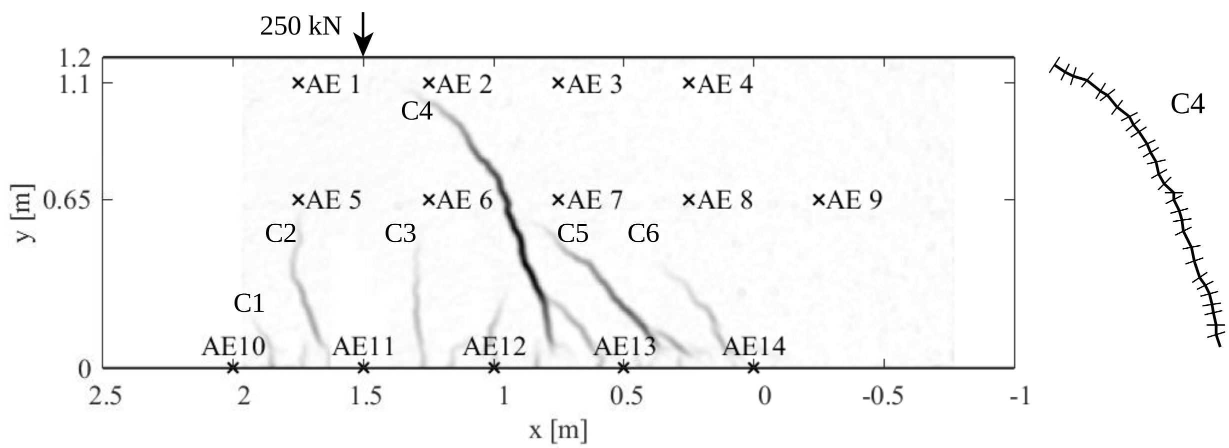


**Figure 3: DIC measurement: (left) crack pattern at 250 kN, and (right) measuring points for the opening of C4 (the short line at each point shows the normal opening direction.)**

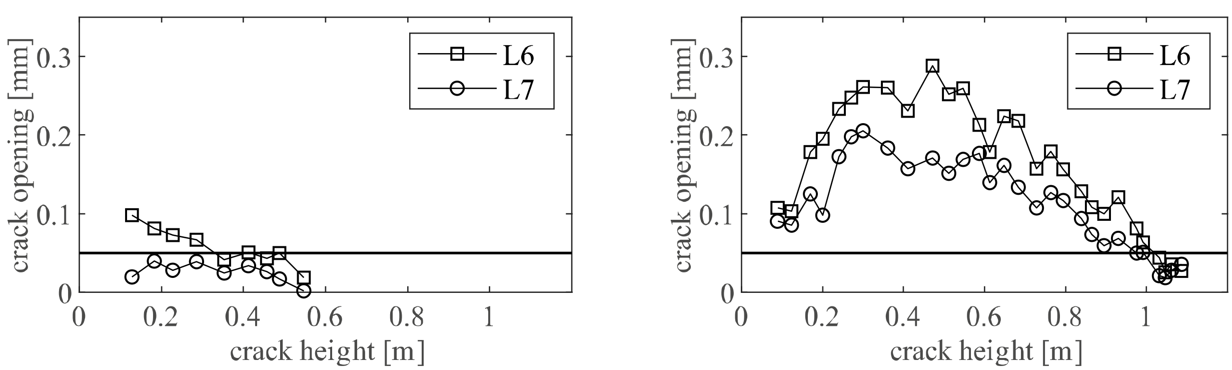


**Figure 4: opening of existing cracks C3 (left) and C4 (right) in the loading process of L6 and L7**

## 4.2 AE source localization in the unloading

The AE activity during unloading was observed to be more active than that during loading in L6 and L7 (shown in Figure 2). This meets with the expectation that for the damaged beam with a higher previous load (in this case, 250 kN in L5), in the cyclic loading of a smaller load level, more AE activities were generated due to the closure of the cracks during unloading.

Grid search method was applied to do the source localization, with the target area (i.e. 2500 mm × 1200 mm) divided by a mesh with a size of 5 mm. Sources located outside the sensor enclosed area had less localization accuracy [8] and were neglected in this work.

The AE source localization results during unloading in L6 and L7 are shown in Figure 5. Each point represents one localized AE activity. It can be seen that AE activities were mostly localized around the cracks C2, C4 and C5, while the cracks C3 and C6 could not be traced back. This may due to the fact that C3 and C6 were opened limitedly in L6 and L7, observed from DIC measurements (the maximum opening of C3 is shown to be less than 0.1 mm in Figure 4, C6 not shown). The closure of these narrow cracks may generate weak signals which could not be received by the AE sensors after attenuation in the propagation. Other cracks which were not reaching the neutral axis could not be detected due to the same reason. It can also be found that the crack C4 was traced back with a higher crack height in L6 than in L7, which met with the DIC measurements.

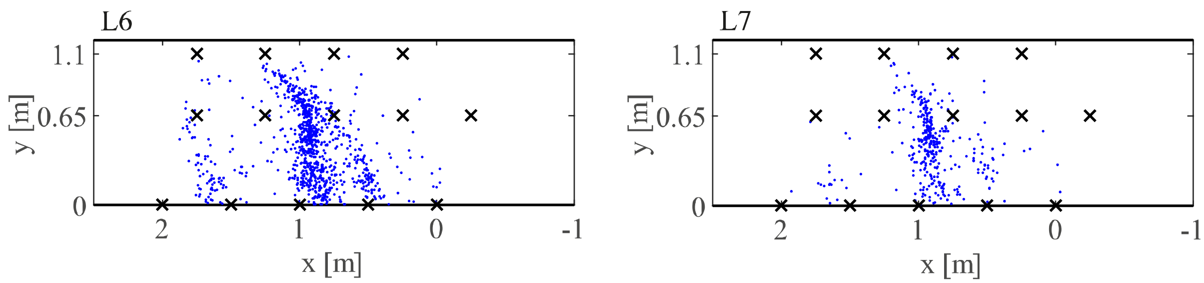


**Figure 5: AE source localization in the unloading process: (left) L6 and (right) L7**

In order to indicate the crack opening along its trajectory, the local AE activities during unloading was calculated. The target area was discretized by cells of size of 80 mm × 80 mm and the number of AE activities located in each cell was counted. The results are illustrated in Figure 6. The cumulative AE activities ranged from 0 to 40 in each cell. The crack opening measured by DIC is shown on the same graph with a scale of 250 times for comparison.

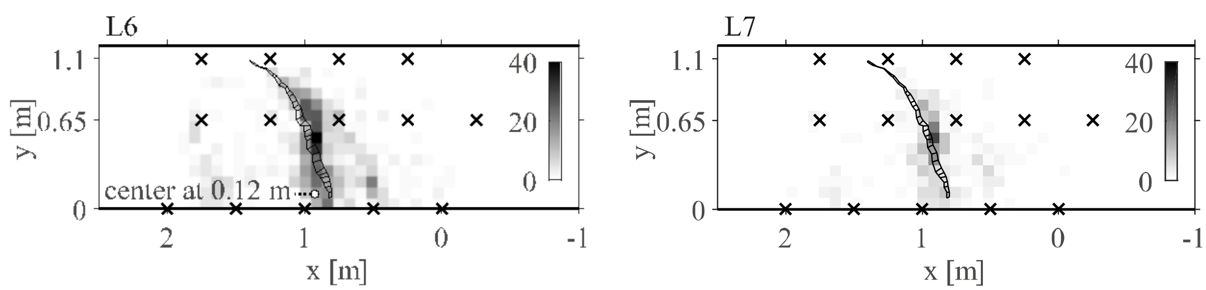


**Figure 6: local cumulative AE activities during unloading in: (left) L6 and (right) L7, compared with the crack opening of C4 from DIC; the center of AE clustering around C4 at 0.12- m height is marked in L6**

By comparing the local cumulative AE activities with the crack opening along the trajectory of the crack C4, it can be found that cells at heights in range of [0.3 0.65] m had more AE activities, where larger crack openings were observed. An initial conclusion can be drawn that in the cyclic loading, the local cumulative AE activities during unloading proportionally corresponded with the crack opening in the previous loading. It can therefore be used as a local indicator of the crack opening along its trajectory. A further quantitative relationship will be reported in another paper with test data from more specimens.

Regarding to the accuracy of AE based crack tracking, the crack tip of C4 can be tracked with a higher accuracy than the bottom part of the crack. If assuming the center of AE clustering as the crack center, the bottom part of the crack C4 was located with an error of around 16 cm (two cells) to the left of DIC result, shown in Figure 6, left. This error came from the influence of the secondary crack between the source and the receiver, combined with the influence of arrival time picking error from the threshold crossing method. More cracks between the source and the receiver can result in larger crack tracking errors. Additional considerations need to be taken.

## 5. CONCLUSIONS

This paper explores the possibility of using local cumulative AE activities during unloading to track the crack pattern in reinforced concrete beams with no further destruction. By comparing with the physical damage in terms of crack opening measured by DIC, several conclusions can be drawn:

- In the performed test in this paper, the local cumulative AE activities during unloading is able to track the trajectory of the cracks with the maximum normal opening larger than 0.1 mm. The closure of narrow cracks less than 0.1 mm may not be detected by the sensors within 0.5 m.
- With an existing crack between the source and the receiver, the accuracy of the AE based cracking tracking has a reduction of around 16 cm. With multiple cracks, additional considerations have to be taken when applying this method.
- The local cumulative AE activities during unloading turns out to be proportionally related to the local normal crack opening from previous loading. The relationship between the cumulative AE activities and the crack opening in a local scale will be quantified in another paper with more test data from various beams.

## 6. REFERENCE LINKING


1. Grosse, C.; Ohtsu, M. *Acoustic emission testing: Basics for research-applications in civil engineering*. 2008; p 1-404, 3540698957.
2. Schechinger, B.; Vogel, T. Acoustic emission for monitoring a reinforced concrete beam subject to four-point-bending. *Construction and Building Materials* 2007, *21*, 483-490.
3. Yang, Y.; Hordijk, D.A.; de Boer, A. Acoustic emission measurement in the proof loading of an existing bridge affected by asr. In *5th International Symposium for Life-Cycle Civil Engineering*, Delft, 2016.
4. Yang, Y.; Hordijk, D.A.; de Boer, A. Acoustic emission study on 50 years old reinforced concrete beams under bending and shear tests. In *8th International Conference on Acoustic Emission*, Kyoto, 2016.
5. Ohtsu, M.; Uchida, M.; Okamoto, T.; Yuyama, S. Damage assessment of reinforced concrete beams qualified by acoustic emission. *ACI Structural Journal* 2002, *99*, 411-417.
6. Ohtsu, M. Recommendation of rilem tc 212-acd: Acoustic emission and related nde techniques for crack detection and damage evaluation in concrete: Test method for damage qualification of reinforced concrete beams by acoustic emission. *Materials and Structures/Materiaux et Constructions* 2010, *43*, 1183-1186.
7. Tobias, A. Acoustic-emission source location in two dimensions by an array of three sensors. *Non-Destructive Testing* 1976, *9*, 9-12.
8. Zhang, F. Evaluation of acoustic emission monitoring of existing concrete structures. Master Thesis, Delft University of Technology, the Netherlands, 2017.